ELSEVIER

Journal of Molecular Catalysis A: Chemical 176 (2001) 151–163

JOURNAL OF MOLECULAR CATALYSIS A: CHEMICAL

www.elsevier.com/locate/molcata

Studies on anion-promoted titania 3. Effect of concentration and source of phosphate ion, method of preparation, and activation temperature on redox, acid–base, textural and catalytic properties of titania

Santosh Kumar Samantaray, Kulamani Parida*

Regional Research Laboratory (CSIR), Bhubaneswar 751013, Orissa, India

Received 9 January 2001; received in revised form 30 March 2001; accepted 25 May 2001

Abstract

The effect of phosphate concentration, source of phosphate ion, method of preparation and activation temperature on the redox, acid–base, textural, and catalytic properties of phosphated titania (PO_4^{3-}/TiO_2) toward alcohol and cumene conversion reactions has been described. The characterisation of the catalyst was performed using X-ray powder diffraction (XRD), infra-red spectroscopy (IR), thermal analysis (TG–DTA), nitrogen adsorption–desorption methods, surface redox, acid–base and phosphate content by spectrophotometric method. TG–DTA and XRD patterns show that phosphate stabilises the anatase phase of TiO_2 up to 1173 K and decreases its crystallite size. IR result shows that phosphate species strongly bound bidentately on TiO_2 supports. Surface area is found to increase with the increase in phosphate content up to 7.5 wt.% loading and thereafter decreases. However, total acidity and the catalytic activity increases with the increase in phosphate content up to 10.0 wt.%. Phosphated samples (pH = 3) prepared using H_3PO_4 as the source of phosphate ion exhibit higher acidity than the samples (pH = 7) using H_3PO_4 and $(NH_4)_3PO_4$, though all the three samples contain same amount of phosphate ion (10.0 wt.%). Among the 573, 773, 973, and 1173 K activated samples, the 573 K sample has shown maximum activity toward the above reactions.

Keywords: Phosphated titania; Alcohol dehydration; Cumene conversion

1. Introduction

The use of titania as a catalyst or catalyst support has been gaining importance day by day due to unique properties, such as acidic, basic, redox sites, thermal shock resistance capacity, ionic conductivity, chemical inertness, and metal support interaction. Recently, much attention has been paid to prepare super-acid titania for many industrially important acid demanding reactions, such as skeletal isomerisation of *n*-alkane, esterification of mono-carboxylic acid and alkylation of aromatics [1–4]. Several industrial heterogeneous catalysts contain phosphoric acid or phosphate and pyrophosphate ions together with oxide phases. The so-called "solid phosphoric acid" (phosphoric acid impregnated on silica or kieselguhr) is a typical acidic heterogeneous catalyst widely used in industry for many years for olefin hydration to alcohols, propylene oligomerisation, alkylation and double-bond isomerisation of 1-butene and disproportionation of CCl_2F_2

* Corresponding author. Tel.: +91-674-481636; fax: +91-674-581637.
E-mail address: kmparida@yahoo.com (K. Parida).

1381-1169/01/$ – see front matter
PII: S1381-1169(01)00247-3

[5–8]. From the preliminary study, it has been shown that incorporation of phosphate ion in TiO_2 enhances important catalytic properties, like stabilisation of surface area, crystal phase, and improvement in surface acidity [9]. Unlike sulphated titania, neither literature is available on PO_4^{3-}/TiO_2 nor it has been studied in detail. However, the use of phosphoric acid or metal phosphates is reported to be added as a dopant to several catalysts, such as in silica, zirconia, alumina, alumina-supported NiW, CoMo HDS and HDN catalysts [10–16]. The role of phosphate species either as a support stabiliser or as a chemical promoter is still not known in detail [17,18].

Acid–base and redox properties are one of the more important types of surface chemical properties of metal oxide catalysts. From a catalytic point of view, TiO_2 possesses a unique type of surface involving both redox and acid–base sites. In addition to high thermal stability, its amphoteric character makes titania a promising catalytic material. The textural and acid–base properties of titania depend greatly on method of preparation, concentration of promoting elements, source of phosphate ion and activation temperature.

In order to understand the generation of surface redox and acidity–basicity, we have prepared TiO_2 at different methods and impregnated by varying the source and concentration of phosphate ion. The PO_4^{3-}/TiO_2 samples are calcined at different temperature and its activity and selectivity toward alcohol and cumene conversion reactions are studied. The results of the reactions are well explained and correlated to the total acidity–basicity and the nature of the sites (Lewis/Brönsted) present on the samples.

2. Experimental

2.1. Materials and methods

Hydrated titania were prepared at pH = 7 and 3 by adding 1:1 ammonia and water to the stirred aqueous solution of titanium tetrachloride, respectively. Obtained gels were filtered and washed repeatedly to remove Cl^- (negative $AgNO_3$ test), dried at 383 K for 10 h, powdered to 45–75 μm mess size and kept for phosphate impregnation. A series of phosphated titania samples were prepared using $(NH_4)_3PO_4$ as a source of phosphate ions by solid–solid kneading method. The other series of phosphated titania samples were prepared by aqueous impregnation method using dilute H_3PO_4. The suspended mass was evaporated to dryness on a hot plate while stirring.

After impregnation with phosphate, the samples were dried in an air oven at 383 K and subsequently calcined at 573, 773, 973, and 1173 K for activation in a muffle furnace. Then the samples were allowed to equilibrate with air, kept in an airtight bottle and stored in desiccator for further use.

3. Characterisation

3.1. Determination of phosphate content

The concentration of phosphate ion in the above samples was measured using UV–VIS spectrophotometer following the ascorbic acid reduction method [19].

3.2. Powder XRD study

The X-ray powder diffraction (XRD) patterns of all the samples were recorded on a Phillips (model: 1710) semiautomatic diffractometer using a Cu Kα radiation source and Ni filter in the range of $2\theta = 10$–80° at a scanning speed of 2°/min. The instrument was operated at 40 kV and 20 mA. The average crystallite size (L) of the particle was determined by XRD line broadening technique using a Scherrer equation:

$$L = \frac{0.94\lambda}{b\cos\theta}, \quad (1)$$

where λ is the wavelength of X-ray used, and b the relative peak broadening, calculated as $b^2 = b_{\text{exp}}^2 - b_{\text{ref}}^2$, where b_{exp} and b_{ref} are half-widths observed on a given sample and on a reference material, which is ideally crystalline, respectively.

3.3. FT-IR study

The infra-red (IR) spectra of unmodified and phosphate-modified TiO_2 samples were recorded with a Perkin-Elmer (model: Paragon 500) FT-IR spectrometer in the range of 4000–400 cm^{-1} on pelletised with KBr phase (spectrophotometric grade).

All the samples were degassed at 383 K in vacuum (1×10^{-4} Torr) before analysis. However, after 383 K evacuation in vacuum, the samples were only retained the ligated water.

3.4. TG–DTA analysis

TG–DTA analyses of 383 K dried samples were carried out in dry air (50 cm^3/min) using a Shimadzu DT-40 thermal analyser in the range of 300–1273 K at a heating rate of 283 K/min.

3.5. Textural properties

Surface area (BET), average pore radius, and pore size distribution were determined by the N_2 adsorption–desorption method at liquid nitrogen temperature using quantasorb (Quantachrome, USA). Prior to adsorption–desorption measurements, the samples were degassed at 393 K and 10^{-4} Torr for 5 h.

3.6. Chemical surface properties

Surface acidity and basicity were determined by the spectrophotometric method [20] on the basis of irreversible adsorption of organic bases, such as pyridine ($pK_b = 8.7$), morpholine ($pK_b = 5.67$), piperidine ($pK_b = 2.90$), and acidic substrates, such as acrylic acid ($pK_a = 4.2$) and phenol ($pK_a = 9.9$). One-electron donor and one-electron acceptor properties were determined on the basis of irreversible adsorption of 1,3-dinitrobenzene (MDNB; electron affinity, EA = 1.26 eV) and phenothiazine (PNTZ; ionisation energy, IE = 7.13 eV) using the same spectrophotometric method.

In all cases, adsorption was carried out from the cyclohexane solution at room temperature. With this method, 10 ml of freshly prepared substrate (0.005–0.01 mol/dm^3) in cyclohexane (AR, Merck) was pipetted into 50 ml stoppered glass conical flasks and then 0.1 g of catalyst dried again at 393 K was added into the flask. The flasks were shaken at constant temperature (298 K) for 2 h by a thermostatic shaker (Julabo, model SW20C) and then the contents were filtered. The absorbance of the filtrate was measured at wavelengths of maximum absorbance (E_{max}). In all cases, sorption experiments were carried out in the concentration ranges of adsorbate where Beer–Lambert's law is valid. The time required for the sorption to reach equilibrium at 298 K was checked for all the samples and was found to never be more than 2 h. All the absorbance measurements were carried out with a Cary-1E (Varian) recording UV–VIS spectrophotometer using 10 mm matched quartz cells.

Once the adsorption remains constant, it is assumed that a monolayer has been formed. As such, the chemical interaction between the adsorbate and catalyst surface may be accompanied by the linear transformed Langmuir adsorption isotherms:

$$\frac{C}{X} = \frac{1}{bX_m} + \frac{C}{X_m}, \tag{2}$$

where C is the concentration of the organic substrate in solution in equilibrium with the adsorbed substrate, b a constant, X the amount of adsorbed substrate per gram of solid, and X_m the monolayer coverage which corresponds to the theoretical amount of solute to cover all of the 1.0 g of solid sample. This method is capable of providing reasonable data on the total concentration of sites as well as the presence of weak and strong acid–base sites.

3.7. Catalytic activity

Catalytic activity of all the samples for dehydration/dehydrogenation of 2-propanol was studied using a fixed-bed catalytic reactor (10 mm i.d.) with on-line GC. Prior to reaction, catalysts were preheated in nitrogen atmosphere at 673 K for 1 h. Alcohol was supplied to the reactor by bubbling nitrogen gas through the alcohol container at 303 K. To avoid condensation of liquid products in the apparatus, all the connections from the reactor to GC were heated at 393 K by heating tape. Reaction products were analysed by means of GC (CIC, India) in FID mode using Porapak Q columns.

The cumene cracking/dehydrogenation reaction was carried out in a micropulse reactor (Sigma, India) using nitrogen as the carrier gas in the temperature range of 673–873 K. Prior to the experiment, the catalyst was activated at 573 K for 1 h in nitrogen stream. The volume of one cumene pulse was maintained at 1 μl. All the products were analysed by GC using a 10 ft SS column with 10% TCEP.

Table 1
Phosphate concentration and BET surface area of PO_4^{3-}/TiO_2 samples activated at different temperatures

Sample no.	Sample code	Concentration of phosphate[a] (wt.%)				
		383 K	573 K	773 K	973 K	1173 K
1	TiO_2	0 (287)	0 (131)	0 (57)	0 (13)	0 (3)
2	2.5P-TiO_2	2.48 (318)	2.59 (192)	2.92 (108)	2.90 (32)	2.85 (10)
3	5.0P-TiO_2	4.95 (346)	5.20 (262)	5.51 (119)	5.55 (51)	5.50 (12)
4	7.5P-TiO_2	7.47 (353)	7.62 (273)	8.20 (158)	8.22 (57)	8.20 (14)
5	10.0P-TiO_2	9.98 (303)	10.18 (258)	11.18 (139)	11.20 (34)	11.18 (11)
6	7.5P-TiO_2(H)[b]	7.49 (315)	7.51 (252)	8.02 (152)	8.03 (32)	8.01 (12)
7	10.0P-TiO_2(H)[b]	9.98 (302)	10.06 (244)	11.04 (136)	11.03 (31)	11.01 (11)
8	7.5P-TiO_2(H*)[c]	7.46 (471)	7.52 (392)	8.04 (173)	8.05 (52)	8.03 (18)
9	10.0P-TiO_2(H*)[c]	9.95 (395)	10.08 (356)	11.04 (155)	11.05 (48)	11.03 (17)

[a] Data in parentheses denote the surface area (BET) in m^2/g.
[b] H_3PO_4-impregnated samples.
[c] H_3PO_4-impregnated samples prepared at pH = 3.

4. Results and discussion

The phosphate concentration of the samples dried at 383 K and after being activated at 573, 773, 973, and 1173 K are shown in Table 1. The concentration of phosphate ion in the samples are seen to increase with increase in activation temperature from 383 to 773 K and after that it remained almost constant till 1173 K. The reason for the initial increases in the wt.% of phosphate with increases in the activation temperature of the samples can be assumed due to loss of water by dehydration.

The powder X-ray diffraction patterns of samples activated at 573, 773, 973, and 1173 K are shown in Figs. 1–3, respectively. It can be seen that samples prepared at pH = 7 with very low or without any phosphate crystallised at 573 K, while the samples prepared at pH = 3 crystallised at higher temperatures (>773 K). From the XRD pattern (Fig. 2, 973 K), it has been found that phosphate ion stabilises the anatase phase of titania. However, samples without any phosphate possess mixture of anatase and rutile phases. It is also observed that (Fig. 3) when samples without phosphate activated at 1173 K possess only rutile phase. However, samples with phosphate possess mixture of anatase and rutile phases. There is no indication of titanium phosphate formation in any one of the samples. To develop a better understanding of formation and crystallisation in the presence of phosphate ion, the average crystallite size (L) perpendicular to the 2 1 0 plane was calculated from XRD patterns of pure titania, as well as phosphated titania. It is seen that the crystallite size of titania decreases with 2.5 wt.% PO_4^{3-} loading and thereafter it remains the same. However, the effect is more pronounced with phosphoric acid as the source of phosphate compared

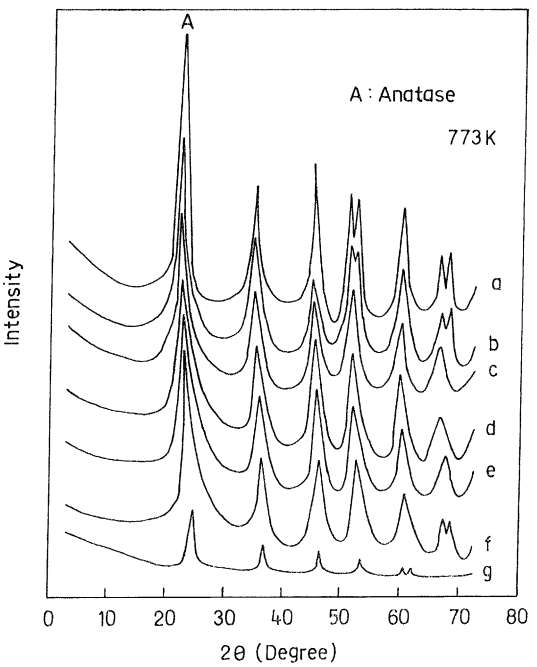

Fig. 1. Powder XRD patterns of phosphated titania samples activated at 773 K: (a) TiO_2; (b) 2.5P-TiO_2; (c) 5.0P-TiO_2; (d) 7.5P-TiO_2; (e) 10.0P-TiO_2; (f) 10.0P-TiO_2(H); (g) 7.5P-TiO_2(H*).

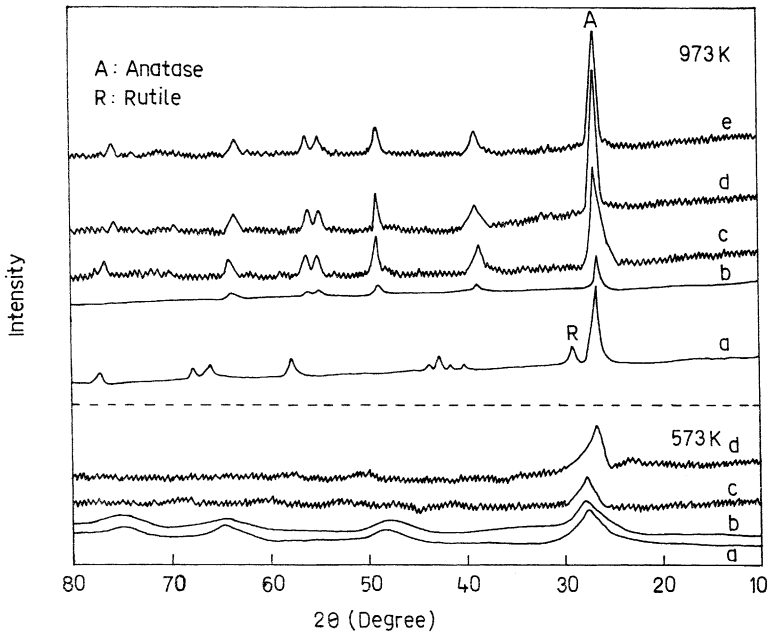

Fig. 2. Powder XRD patterns of phosphated titania samples — activated at 573 K: (a) TiO_2; (b) 2.5P-TiO_2; (c) 10.0P-TiO_2; (d) 10.0P-TiO_2(H); activated at 973 K: (a) TiO_2; (b) 2.5P-TiO_2; (c) 10.0P-TiO_2(H*); (d) 10.0P-TiO_2(H); (e) 10.0P-TiO_2.

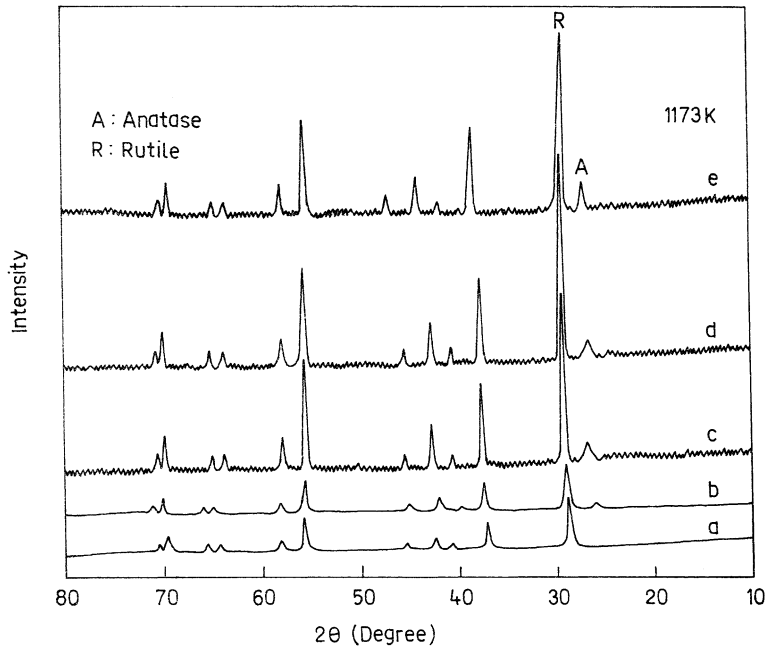

Fig. 3. Powder XRD patterns of phosphated titania samples activated at 1173 K: (a) TiO_2; (b) 2.5P-TiO_2; (c) 10.0P-TiO_2(H*); (d) 10.0P-TiO_2(H); (e) 10.0P-TiO_2.

to $(NH_4)_3PO_4$. This indicates that the crystallinity is more or less dependent on the presence of phosphate ion, but not on the source and percentage of phosphate loading. In addition to stabilising anatase TiO_2 crystallites, phosphate surface species inhibit TiO_2 crystallite sintering, leading to smaller crystallites than in pure TiO_2. The crystallite size decreases in the presence of phosphate ions as PO_4^{3-} species could possibly interact with TiO_2 network, and thus hinder the growth of the particle. Even a very small amount of PO_4^{3-} species is responsible for this effect. Therefore, the change in phosphate concentration did not change crystallite size further. Therefore, it is assumed that small amount of phosphate species is responsible for the lowering of crystallite size. From Fig. 4, it is observed that crystallite size increases with increase in activation temperature from 573 to 773 K and thereafter it decreases. The former may be due to desorption of surface hydroxyl group from the TiO_2 network and the latter is due to the formation of rutile phase as well as inhibits sintering. This suggests that phosphate species strongly interacting with TiO_2 crystallites inhibit sintering even at high activation temperatures. This type of effect is also observed in

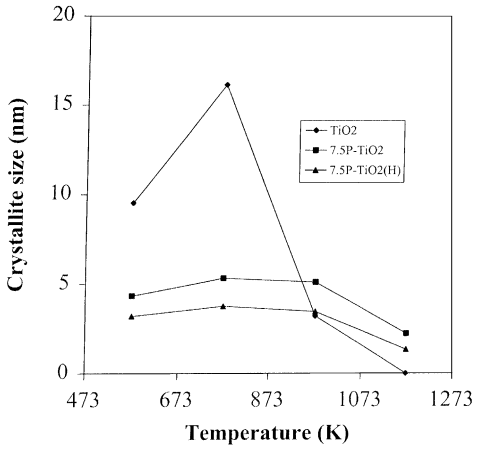

Fig. 4. Average crystallite size of samples activated at different temperatures.

PO_4^{3-}-modified FeO(OH) [21], WO_3-modified ZrO_2 [22] and TiO_2 [23].

The IR absorption spectra of the unmodified and phosphated titania samples activated at different temperatures are shown in Fig. 5. The bands at 3430 and 1630 cm^{-1}, possessed by all the samples even after

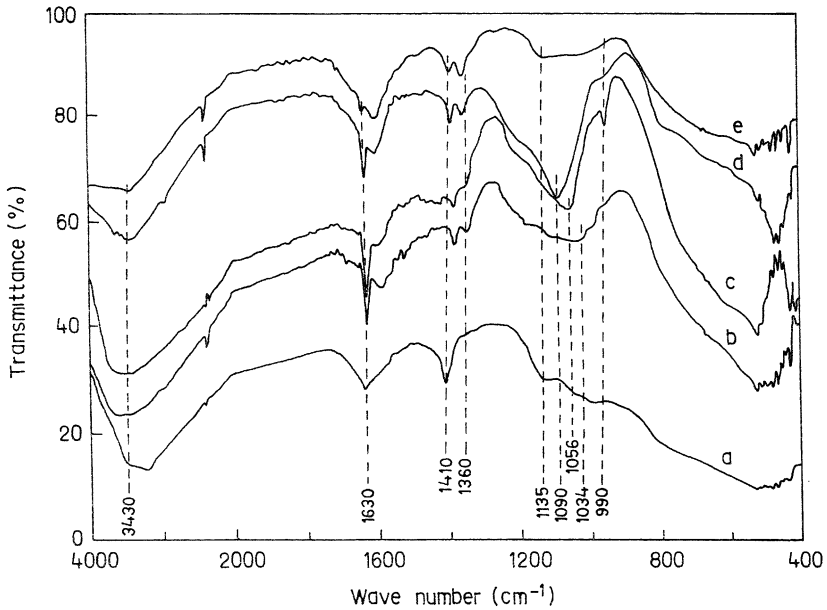

Fig. 5. FT-IR spectra of (a) 10.0P-TiO_2(H*) at 773 K, and 10.0P-TiO_2 samples activated at (b) 573 K, (c) 773 K, (d) 973 K, and (e) 1173 K, respectively.

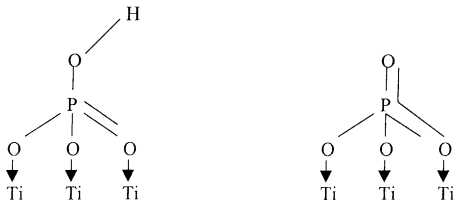

Scheme 1.

activated at 773 K, correspond to the specificity for OH stretching and bending vibrations, respectively. This absorption band assigned to the strongly H-bonded H–O–H species may be due to the residual surface hydroxyl groups/ligated H_2O in the samples. Infra-red spectra of phosphated metal oxide generally show a strong sharp absorption band at 1300–1450 cm^{-1} and broad bands at 950–1150 cm^{-1}. The 1300–1450 cm^{-1} peak is the stretching frequency of P–O bonds whose order is close to two (P=O, phosphoryl groups) and the 950–1150 cm^{-1} peaks are the characteristic frequencies of PO_4^{3-}. The broad bands at 950–1150 cm^{-1} resulted from the lowering of the symmetry in the free PO_4^{3-} (Td point group). The PO_4^{3-} is bound to the titania surface, the symmetry can be lower to either C_{3V} or C_{2V} [24]. Here, the band that splits into three peaks (1056, 1034, 990 cm^{-1}) were assigned to the bidentately bound phosphate ion (C_{2V} point group). These three bands somewhat shifted to higher wave number (1090 and 1135 cm^{-1}) when the sample is activated above 973 K and sample prepared at pH = 3. This agrees with the position of such a fundamental band, as has been directly observed in the case of phosphated zirconia [25] and alumina [26]. The above results give several indications of the structure of the phosphate species supported on the titania supports. Based on the main IR features discussed above, the surface structures are reported in Scheme 1.

The simultaneous TG and DTA curves of the unmodified and phosphate-modified samples are performed in air. The samples undergo consistent weight loss below 573 K due to desorption of water molecules. Successively, a slight continuous weight loss is observed until 873 K for phosphated sample and until 973 K for unmodified sample. The absence

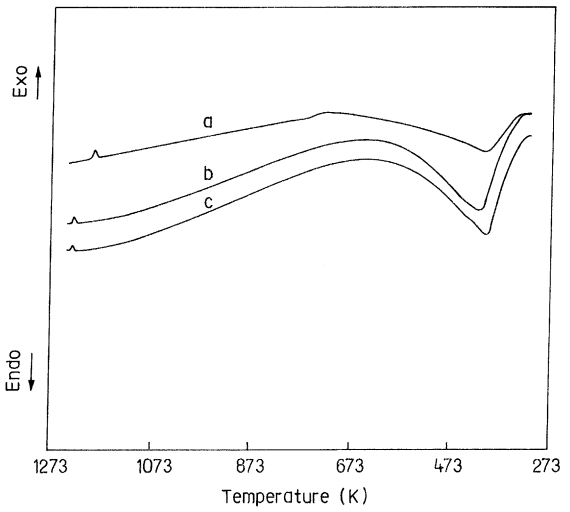

Fig. 6. Differential thermal analyses of samples: (a) TiO_2; (b) 10.0P-TiO_2; (c) 10.0P-TiO_2(H).

of relevant weight loss above 873 K in case of phosphated samples would also indicate that phosphate ion is rather strongly bonded to the support and does not desorb nor evaporate on heating. Desorption of water corresponds to endothermic peak in the DTA curves (Fig. 6). The exothermic peak observed very clearly for phosphate-modified titania and, to a lower extent, for unmodified titania in the region near 1173 K without any corresponding weight loss is due to solid-state transformations (anatase to rutile transformation). This result is further supported by XRD analysis. Its position at so high a temperature that agrees with the inhibiting effect of phosphate species on the anatase to rutile transformation already reported [27].

The values in parentheses (Table 1) show the BET surface area of the samples in square meters per gram. With the increase in phosphate content from 0 to 7.5 wt.%, the surface area of the materials increases from 287 to 353 m^2/g in case of 383 K dried samples. However, at 10.0 wt.% PO_4^{3-}, the surface area decreases to 303 m^2/g. The same trends are observed irrespective of the source of phosphate ion, method of preparation and for samples activated at different temperatures, i.e. 573, 773, 973, and 1173 K. This implies that the presence of PO_4^{3-} ions plays a role in making the material porous. However, when the phosphate content increases beyond 7.5 wt.%, pore blocking takes place due to the presence of an excess

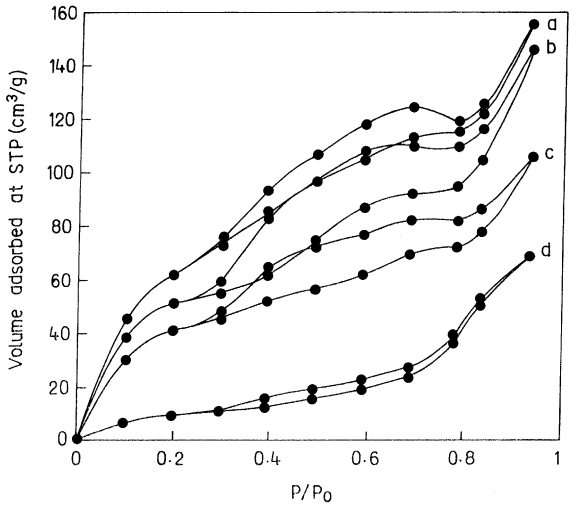

Fig. 7. Nitrogen adsorption–desorption isotherms of 7.5P-TiO_2 samples activated at: (a) 573 K; (b) 773 K; (c) 973 K; (d) 1173 K.

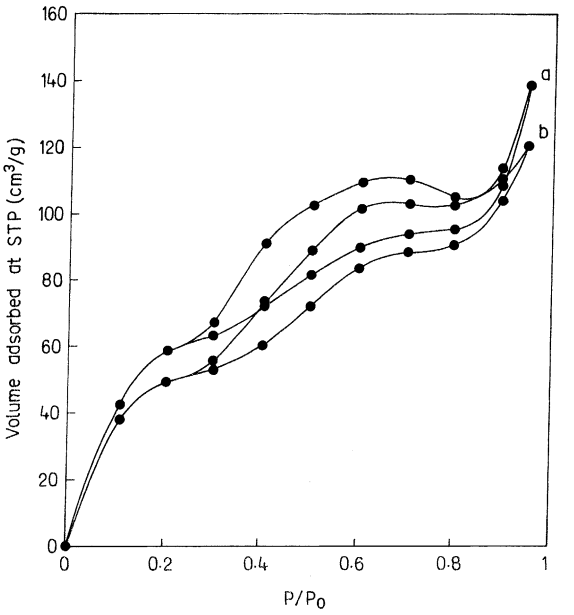

Fig. 8. Nitrogen adsorption–desorption isotherms of (a) 7.5P-TiO_2(H) and (b) 7.5P-TiO_2(H^*) samples activated at 773 K.

amount of phosphate. This type of observation was also noted in case of phosphated zirconia [12]. With increase in activation temperature, the surface area decreases gradually. This might be due to the inter-particle agglomeration or due to collapse of very fine/narrow pores. It is also observed that the sample prepared at pH = 3 has higher surface area compared to the sample prepared at pH = 7.

The nitrogen adsorption–desorption isotherm of some representative samples are shown in Figs. 7 and 8. All of the curves are nearly of same type and can be assigned as type IV or II in the BDDT classification [28]. From the shape of the curves, it can be predicted that samples activated at 1173 K consist of mainly mesopores. However, samples with varying source of phosphate ion and method of preparation are micro-mesopores. A similar observation can also be drawn from the pore size distribution curves (Fig. 9) calculated by BJH equation [29]. So due to the microporosity, samples prepared at pH = 3 show a very high surface area. The *t*-plots (Fig. 10) of samples activated at different temperatures (up to 973 K), varying source of phosphate ion and method of preparation show a downward deviation, except for sample activated at 1173 K. The downward deviation reveals that these samples contain predominantly micropores along with some mesopores, whereas an upward deviation indicates the presence of mesopores. The

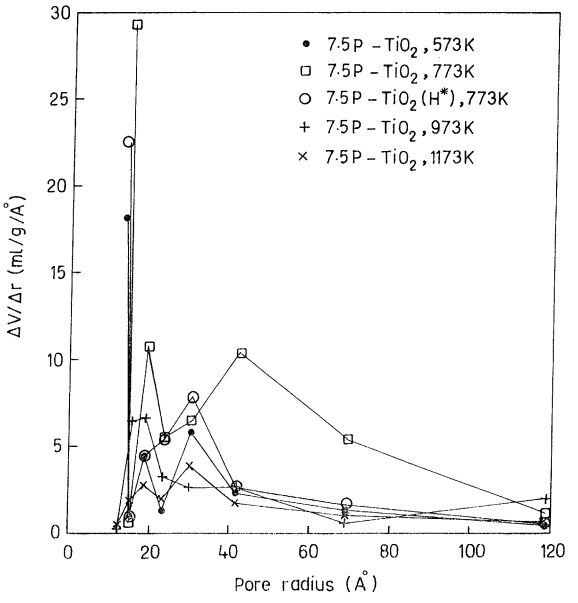

Fig. 9. Distribution of pores as a function of pore radius.

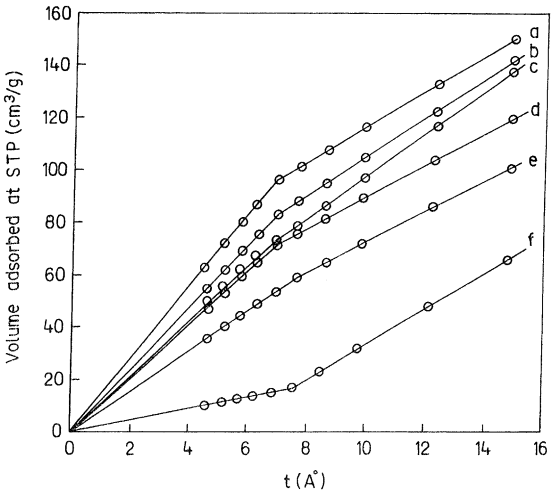

Fig. 10. The *t*-plots of samples: (a) 7.5P-TiO_2 at 573 K; (b) 7.5P-TiO_2 at 773 K; (c) 7.5P-TiO_2(H) at 773 K; (d) 7.5P-TiO_2(H*) at 773 K; (e) 7.5P-TiO_2 at 973 K; (f) 7.5P-TiO_2 at 1173 K.

upward deviation pore samples activated at 1173 K may be explained by an enhanced adsorption due to capillary condensation into mesopores 4–10 nm in diameter [30].

The total acidity measured by the adsorption of piperidine, strong acid sites by pyridine, and moderate acid sites by morpholine all gradually increased with increase in phosphate wt.% up to a value of 10.0 (Table 2). This indicates that all types of acid sites are present in phosphated titania. It is observed that phosphated samples prepared using phosphoric acid as the source of phosphate ion exhibit higher acidity compared to the sample prepared using ammonium phosphate. It is also observed that PO_4^{3-}/TiO_2 samples prepared at pH = 3 exhibit higher acidity compared to the PO_4^{3-}/TiO_2 samples prepared at pH = 7. It is reasonable to assume that during the preparation procedure, the aqueous phosphoric acid protonates all types of titania hydroxyls by an acid–base reaction. However, phosphate of ammonium phosphate by solid–solid leading method undergoes interaction with all types of basic hydroxyls to a smaller extent, resulting in less acidity compared to the phosphate of phosphoric acid by aqueous impregnation method. Similar observations have been reported earlier in case of SO_4^{2-} [31] and PO_4^{3-} [32] on alumina. It can be seen from Table 2 that with increase in activation temperature from 573 to 1173 K, the acid sites are found to decrease due to the loss of bonded hydroxyl groups.

The total basicity measured by the adsorption of acrylic acid and strong basic site by phenol is presented in Table 3, from which it can be seen that the changed surface basic sites with respect to the source of phosphate ion, method of preparation and activation temperature exhibit the same trend as acid sites. With increase in phosphate concentration, the basic sites gradually decrease.

Table 4 represents the redox sites of phosphated titania. The oxidising and reducing properties are determined by the adsorption of *m*-dinitrobenzene (MDNB) and PNTZ, respectively. From the data, it can seen that electron donocity of both the unmodified and phosphate-modified titania decreases with increase in

Table 2
Surface acidity of the PO_4^{3-}/TiO_2 samples activated at different temperatures[a]

Sample no.	Surface acid sites (μmol/g)											
	Piperidine (pK_b = 2.90)				Morpholine (pK_b = 5.67)				Pyridine (pK_b = 8.70)			
	573 K	773 K	973 K	1173 K	573 K	773 K	973 K	1173 K	573 K	773 K	973 K	1173 K
1	1012	260	210	102	697	143	117	41	233	100	46	7
2	1088	360	305	171	769	280	257	128	319	202	88	12
3	1163	401	390	241	903	325	271	215	374	220	109	18
4	1281	445	408	295	914	340	315	245	400	264	129	19
5	1331	497	482	305	992	361	383	266	444	299	182	21
6	1229	466	425	317	1002	351	403	367	431	273	172	20
7	1458	602	515	325	1109	445	421	393	456	377	255	25
8	1598	944	–	–	1170	665	–	–	505	407	–	–
9	1602	964	–	–	1485	727	–	–	512	503	–	–

[a] Activation at 573 K, 773 K, 973 K, and 1173 K.

Table 3
Surface basicity of the PO_4^{3-}/TiO_2 samples activated at different temperatures[a]

Sample no.	Surface basic sites (μmol/g)							
	Acrylic acid ($pK_a = 4.2$)				Phenol ($pK_a = 9.9$)			
	573 K	773 K	973 K	1173 K	573 K	773 K	973 K	1173 K
1	757	383	257	107	354	241	122	62
2	734	377	245	84	341	235	105	52
3	718	368	226	79	335	225	89	47
4	684	349	219	73	327	218	83	45
5	647	345	202	69	317	211	73	40
6	535	266	177	50	257	104	50	24
7	627	303	193	55	284	155	54	25
8	500	253	–	–	214	178	–	–
9	585	298	–	–	221	137	–	–

[a] Activation at 573 K, 773 K, 973 K, and 1173 K.

temperature going through a minimum at 773 K and then increases on heating to 973 K. The initial decrease in electron donocity may be due to the decrease in surface hydroxyl groups with increase in temperature. The increase in electron donocity at 973 K may be due to the increase in number of electrons trapped in defect site, which is another source of electron donor sites in metal oxides. In case of phosphated titania samples, the electron donating capacity decreases, implying that some of the basic sites are converted to acid sites. It is already reported that the mechanism of phosphation is an anion exchange between PO_4^{3-} and OH^- [33]. The electron donating capacity of phosphate-modified titania is almost equal to that of unmodified one when the activation temperature is 973 K, because trapped electrons are solely responsible for basicity at high temperatures. Further, there is no hydroxyl ion for exchange with phosphate ion at high temperatures. However, the electron accepting properties of titania decreases with respect to both phosphate modification and activation temperature.

The 2-propanol conversion produces both propene and acetone as major products, while diisopropyl ether is found as a minor product. In unmodified titania, acetone selectivity is more than propene selectivity. However, with the increase in phosphate contents in the sample, propene selectivity increases (Table 5). On all the catalysts, higher acetone selectivity is found at low temperature. With the increase in propene formation, acetone selectivity drastically decreases. This

Table 4
One-electron donor–acceptor properties of PO_4^{3-}/TiO_2 samples activated at different temperatures[a]

Sample no.	Redox sites (μmol/g)							
	MDNB (EA = 1.26 eV)				PNTZ (IE = 7.13 eV)			
	573 K	773 K	973 K	1173 K	573 K	773 K	973 K	1173 K
1	71	65	98	73	190	69	55	20
2	60	55	73	66	72	79	81	20
3	59	51	71	62	50	53	56	19
4	59	49	70	59	40	50	53	17
5	53	43	66	56	38	48	51	17
6	54	44	65	57	42	52	57	15
7	51	41	62	54	40	49	54	14
8	50	40	–	–	45	55	–	–
9	45	38	–	–	43	50	–	–

[a] Activation at 573 K, 773 K, 973 K, and 1173 K.

Table 5
Conversion (mol%) of 2-propanol over PO_4^{3-}/TiO_2 using nitrogen as carrier[a]

Sample no.	Reaction temperature											
	393 K				433 K				473 K			
	573 K	773 K	973 K	1173 K	573 K	773 K	973 K	1173 K	573 K	773 K	973 K	1173 K
1	2 (0)	0 (0)	0 (0)	0 (0)	4 (0)	0 (0)	0 (0)	0 (0)	8 (96)	2 (90)	1 (76)	0 (0)
2	7 (100)	4 (98)	2 (94)	1 (80)	10 (96)	7 (90)	6 (82)	3 (70)	18 (82)	12 (78)	10 (60)	6 (42)
3	6 (94)	3 (92)	2 (90)	1 (68)	8 (80)	6 (72)	5 (60)	3 (52)	15 (68)	10 (60)	6 (46)	4 (32)
4	5 (58)	2 (52)	1 (48)	0 (0)	7 (28)	5 (24)	5 (18)	2 (12)	13 (10)	9 (6)	4 (4)	3 (0)
5	5 (28)	1 (18)	1 (10)	0 (0)	6 (14)	4 (10)	3 (6)	1 (2)	10 (0)	7 (0)	3 (0)	1 (0)
6	6 (12)	2 (14)	1 (6)	0 (0)	9 (10)	5 (8)	4 (0)	2 (0)	14 (0)	9 (0)	5 (0)	4 (0)
7	8 (8)	2 (12)	1 (4)	0 (0)	12 (6)	5 (4)	4 (0)	2 (0)	18 (0)	10 (0)	8 (0)	6 (0)
8	7 (4)	3 (10)	2 (0)	1 (0)	15 (0)	7 (2)	6 (0)	4 (0)	23 (0)	12 (0)	10 (0)	8 (0)
9	10 (0)	3 (6)	2 (0)	1 (0)	19 (0)	10 (0)	8 (0)	6 (0)	28 (0)	13 (0)	12 (0)	10 (0)

[a] Activation at 573 K, 773 K, 973 K, and 1173 K; values in parentheses represent percentage selectivity to dehydrogenation product.

may be due to the poisoning of the basic sites by the water molecules formed by a dehydration process.

In the case of unmodified titania, acetone formation started at 453 K, while on the 2.5 wt.% phosphated sample, the same reaction starts at 393 K. This drastic decrease in the reaction temperature indicates that the phosphate molecule plays some role in the dehydrogenation process. However, with the increase in phosphate content, acetone selectivity decreases. Therefore, dehydrogenation takes place on the basic sites present in the titania surface. With the increase in the phosphate content, these sites are poisoned by the phosphate molecule [10], thus decreasing the dehydrogenation selectivity. However, the small amount of phosphate probably acts as a promoter for the dehydrogenation reaction, thus decreasing the reaction temperature. Among all the samples, 10.0P-TiO_2(H^*) shows higher propene selectivity. The 2-propanol conversion is highest on 10.0P-TiO_2(H^*), whereas acetone selectivity is more in the case of 10.0P-TiO_2, though both the samples contain the same amount of phosphate. Therefore, it can be interpreted that the surface acid–base sites can be controlled by varying the method of preparation.

Among 573, 773, 973, and 1173 K activation, 573 K activated samples have shown maximum 2-propanol conversion activity followed by 773, 973, and 1173 K activated samples. The selectivity to dehydrogenation product decreased as the activation temperature increased. This is quite similar to surface acidity of the samples which has followed the same trend. From this, we can say that the total conversion of 2-propanol is a function of total acidity.

Table 6 presents the results of the cumene conversion reaction. In the conversion of cumene, two types of reactions occur, i.e. cracking to benzene and propene and dehydrogenation to α-methyl styrene. Table 6 includes both the percentage of total conversion and the benzene to α-methyl styrene ratio (value inside the parentheses). From Table 6, it is found that with the increase in the phosphate content, total cumene conversion increases. A particular sample (pH = 3) prepared from H_3PO_4 exhibits higher conversion than both the samples (pH = 7) prepared from H_3PO_4 and $(NH_4)_3PO_4$, though these samples contain same amount of phosphate (10.0 wt.%). From the benzene to α-methyl styrene ratio, it is well marked that the benzene selectivity is higher at low temperature conversion. With the increase in reaction temperature, α-methyl styrene selectivity increases. In the case of unmodified titania, α-methyl styrene selectivity is more than the benzene selectivity. However, with the increase in phosphate content, benzene selectivity increases at all reaction temperatures. It is known that cracking proceeds over Brönsted acid sites, whereas dehydrogenation occurs on Lewis acid sites. Thus, it can be concluded that the unmodified titania mostly contains Lewis acid sites. With the increase in phosphate impregnation, the number of Lewis acid sites decreases, thus decreasing the α-methyl styrene selectivity.

Table 6
Results of cumene cracking/dehydrogenation (mol%) over PO_4^{3-}/TiO_2[a]

Sample no.	Reaction temperature								
	573 K			673 K			773 K		
	573 K	773 K	973 K	573 K	773 K	973 K	573 K	773 K	973 K
1	1.3 (3.3)	0 (0)	0 (0)	4.2 (5)	3.5 (0.16)	0 (0)	35 (5.3)	30.7 (0.33)	10.2 (0.24)
2	3.3 (7.2)	1.2 (5)	1 (2.3)	15.2 (5.9)	13.5 (2.9)	5.1 (1)	40.2 (5.5)	39 (2.25)	16 (1.6)
3	3.9 (12)	1.7 (7.5)	1.5 (4)	22.2 (9)	20 (4)	14 (3.6)	55.5 (8.2)	48 (3.8)	24 (3)
4	4.8 (23)	2.2 (21)	2 (7)	30 (14)	27.5 (5.1)	19 (4.4)	59 (10.8)	57.5 (4)	30.5 (4)
5	6.0 (29)	4.2 (26.6)	3.6 (17)	31.5 (19.3)	27.5 (5.85)	20 (5.6)	68.6 (18)	66 (5)	32.4 (4.4)
6	7.2 (35)	6.4 (31)	4.4 (20)	33 (32)	28.1 (12.4)	23.5 (8.4)	70.6 (22.5)	68.5 (7)	36 (6.2)
7	12.5 (40.6)	10.3 (33.3)	6 (29)	33.8 (36.5)	28.5 (18.6)	24 (11)	87 (33.8)	85.4 (8.1)	42 (7.4)
8	14 (45.6)	12 (39)	6.6 (32)	35.2 (43)	30.2 (24.1)	26 (16.3)	92.2 (40.9)	88 (10)	52 (9.4)
9	17 (55.6)	15.2 (49.6)	6.9 (45.3)	37 (51.8)	32.6 (31.6)	27.1 (23.6)	94.8 (46.4)	90.2 (17)	58.5 (12)

[a] Activation at 573 K, 773 K, and 973 K; values in parentheses represent the benzene to α-methyl styrene ratio.

With activation temperature of the sample, the total conversion of cumene is as follows: 573 K > 773 K > 973 K. The highest activity of the 573 K activated samples can be correlated with the total surface acidity (Table 2) which is maximum for 573 K activated samples. The lowest activity in case of 973 K activated samples could be due to the decrease in both the surface acidity and surface area of the samples. It is interesting to note that though the activity decreased with increases in the activation temperature, the selectivity to dehydrogenation product increased. Again this reveals that at higher activation temperature, more Lewis acid sites are formed.

5. Conclusions

1. It is found that phosphate impregnation can increase the surface porosity as well as acidity of titania and inhibits sintering at high activation temperatures. On the contrary, basic sites and redox sites decrease with phosphate loading.
2. However, the surface acid–base sites and the presence of Brönsted and Lewis sites varies with the variation in the method of preparation, source and concentration of phosphate ion.
3. Sample prepared at pH = 3 exhibits higher surface area and acid sites, but lower porosity, basic sites and redox sites compared to the sample prepared at pH = 7.
4. The 573 K activated sample exhibits highest acid sites, basic sites and redox sites among other activated samples.
5. Titania prepared at pH = 3 loaded with 10.0 wt.% of phosphate ion (H_3PO_4 as the source of phosphate ion) can be used as an efficient solid acid catalyst for the conversion of 2-propanol to propene and cumene to benzene.

Acknowledgements

The authors are thankful to Dr. V.N. Misra, Director, Regional Research Laboratory (CSIR), Bhubaneswar, for giving permission to publish this paper and to Dr. S.B. Rao, Head, Inorganic Chemicals Division, for his valuable suggestions and constant encouragement. One of the authors, S.K. Samantaray is obliged to CSIR, New Delhi, for a senior research fellowship.

References

[1] A.K. Dalai, R. Sethuraman, S.P.R. Katikaneni, R.O. Idem, Ind. Eng. Chem. Res. 37 (1998) 3869.
[2] L. Rongsheng, C. Jingfeng, Z. Wuyang, Y. Hua, Z. Zhiming, W. Quan, React. Kinet. Catal. Lett. 48 (2) (1992) 483.
[3] S. Sugunan, C.R.K. Seena, Ind. J. Chem. 38A (1999) 947.
[4] S.K. Samantaray, T. Mishra, K.M. Parida, J. Mol. Catal. A 156 (2000) 267.
[5] E.K. Jones, Adv. Catal. 8 (1956) 219.

[6] E. Weisand, P.A. Engelhard, Bull. Soc. Chim. Fr. (1968) 1811.
[7] P. Friedman, K.L. Pinder, Ind. Eng. Chem. Process. Des. Dev. 10 (1971) 548.
[8] A. Hess, E. Kemnitz, Appl. Catal. A 149 (1997) 373.
[9] K.M. Parida, M. Acharya, S.K. Samantaray, T. Mishra, J. Colloid Interface Sci. 217 (1999) 388.
[10] G. Busca, G. Ramis, V. Lorenzelli, P.F. Rossi, Langmuir 5 (1989) 911.
[11] C. Ramis, P.F. Rossi, C. Busca, V. Lorenzelli, Langmuir 5 (1989) 917.
[12] K.M. Parida, P.K. Pattnayak, J. Colloid Interface Sci. 182 (1996) 381.
[13] P.K. Pattnayak, K.M. Parida, J. Colloid Interface Sci. 226 (2000) 340.
[14] M. Jenny, R.A. Kydd, J. Catal. 132 (1991) 465.
[15] C. Morterra, C. Magnacca, P.P. De Maestri, J. Catal. 152 (1995) 384.
[16] P. Berteau, M. Kellens, B. Delmon, J. Chem. Soc., Faraday Trans. 87 (9) (1991) 1425.
[17] C.W. Fitz, H.F. Rose, Ind. Eng. Chem. Prod. Res. Dev. 22 (1983) 40.
[18] K. Gisthi, A. Iannibello, S. Marengo, G. Morelli, P. Tittarelli, Appl. Catal. 12 (1984) 381.
[19] D.J. Rochford, Aust. J. Mar. Fresh Water Res. 2 (1951) 1.
[20] J.M. Campelo, A. Gareia, J.M. Gutierrez, D. Luna, J.M. Marina, J. Colloid Interface Sci. 95 (1983) 544.
[21] K. Kandori, S. Uchida, S. Kataoka, T. Ishikawa, J. Mater. Sci. 27 (1992) 719.
[22] D.G. Barton, S.L. Soled, G.D. Meitzner, G.A. Fuentes, E. Iglesia, J. Catal. 181 (1999) 57.
[23] L.J. Alemany, M.A. Larrubia, M.C. Jimenez, F. Delgado, J.M. Blasco, React. Kinet. Catal. Lett. 60 (1) (1997) 41.
[24] K. Nakamoto, Infra-Red and Raman Spectra of Inorganic and Coordination Compounds, 4th Edition, Wiley, New York, 1986.
[25] G. Ramis, G. Busca, V. Lorenzelli, P.F. Rossi, M. Bensitel, O. Saur, J.C. Lavalley, in: Proceedings of the IXth International Congress on Catalysis, Calgary, Canada, 1988, p. 1874.
[26] A. Mennour, C. Ecolivet, D. Cornet, J.F. Hemidy, J.C. Lavalley, L. Mariette, P. Engelhard, Mater. Chem. Phys. 19 (1988) 301.
[27] J. Criado, C. Real, J. Chem. Soc., Faraday Trans. (I) 79 (1983) 2765.
[28] S. Brunauer, D.W. Demming, L.S. Demming, F. Teller, J. Am. Chem. Soc. 62 (1940) 1723.
[29] E.P. Barrett, L.G. Joyner, P.P. Halonga, J. Am. Chem. Soc. 73 (1951) 373.
[30] S.J. Gregg, K.S.W. Sing, Adsorption, Surface Area and Porosity, 2nd Edition, Academic Press, New York, 1982.
[31] Y. Okamoto, T. Imanaka, J. Phys. Chem. 92 (1988) 7102.
[32] J.M. Lewis, R.A. Kydd, J. Catal. 132 (1991) 465.
[33] J. Navarette, T. Lopez, R. Gomez, Langmuir 12 (1996) 4385.